Radiology Case Reports 18 (2023) 2884–2894

Available online at www.sciencedirect.com

ScienceDirect

journal homepage: www.elsevier.com/locate/radcr

Case Report

Gliomatosis cerebri with blindness: A case report with literature review ☆,☆☆

Amirreza Jahanshahi, MD[a,g], Sareh Salarinejad, MD[b], Saeed Oraee-Yazdani, MD, PhD[c], Yasaman Chehresonboll, MD[d], Soroush Morsali, MD[e], Ali Jafarizadeh, MD, MPH[f], Masih Falahatian, MD[g,], Faezeh Rahimi, MD[h], Mehran Jaberinezhad, MD, MPH[i]*

[a] *Department of Radiology, Emam Reza Hospital, Tabriz University of Medical Sciences, Tabriz, Iran*
[b] *Department of Pathology, Faculty of Medicine, Shohada-e-Tajrish Hospital, Shahid Beheshti University of Medical Science, Tehran, Iran*
[c] *Functional Neurosurgery Research Center, Shohada Tajrish Comprehensive Neurosurgical Center of Excellence, Shahid Beheshti University of Medical Sciences, Tehran, Iran*
[d] *Department of Surgical and Clinical Pathology, Shahid Beheshti University of Medical Sciences, Tehran, Iran*
[e] *Neuroscience Research Center (NSRC), Tabriz University of Medical Sciences, Tabriz, Iran*
[f] *Nikookari Eye Center, Tabriz University of Medical Sciences, Tabriz, Iran*
[g] *Medical Radiation Sciences Research Group, Imam Reza Hosptial, Tabriz University of Medical Sciences, Tabriz, Iran*
[h] *Department of Radiology, Zanjan University of Medical Sciences, Zanjan, Iran*
[i] *Clinical Research Development Unit of Tabriz Valiasr Hospital, Tabriz University of Medical Sciences, Tabriz, Iran*

ARTICLE INFO

Article history:
Received 16 March 2023
Revised 10 May 2023
Accepted 12 May 2023

Keywords:
Gliomatosis cerebri
Glioma
Blindness
Magnetic resonance imaging (MRI)
Magnetic resonance spectroscopy (MRS)
Case report

ABSTRACT

Cerebral gliomatosis (GC) is a rare diffuse infiltrative growth pattern of glioma with non-specific clinical manifestations like visual impairment that may involve bilateral temporal lobes. Herpes simplex encephalitis (HSE) and limbic encephalitis (LE) can also lead to temporal lobe involvement. Differentiating these entities is necessary for patients with misleading presentations and imaging findings. To the best of our knowledge, this is the third case of GC presenting with blindness. The patient was a 35 years-old male in a drug rehabilitation center for heroin addiction. He presented with a headache, a single episode of seizure, and a 2-month history of bilateral decrease in visual acuity, which had acutely worsened. Magnetic resonance imaging (MRI) and computed tomography (CT) showed bilateral temporal lobe involvement. Ophthalmological studies showed bilateral papilledema, absence of visual evoked potential, and thickening of the retinal nerve fiber layer. Due to this clinical presentation, normal laboratory data, and suspicious MRI findings, further investigation with magnetic resonance spectroscopy (MRS) was performed. Results showed a greatly increased ratio of choline to creatinine(Cr) or N-acetyl aspartate (NAA), suggesting a neoplastic

☆ Acknowledgments: We are thankful for the help of Dr Ali Hekmatnia, Dr Farzaneh Hekmatnia, Dr Andrew Parviz Zarei, Dr Seyyed Mojtaba Nekooghadam Motlagh, the entire Imam Reza Hospital Radiology Department, the Neurology Ward, and ICU staff, as well as Shohada-e-Tajrish Hospital ICU staff.
☆☆ Competing Interests: The authors declare that they have no known competing financial interests or personal relationships that could have appeared to influence the work reported in this paper.
* Corresponding author.
E-mail address: Masih.falahatian@gmail.com (M. Falahatian).
https://doi.org/10.1016/j.radcr.2023.05.037

nature of the disease. Subsequently, the patient was referred for a brain tissue biopsy with a suspicion of malignancy. The pathology results revealed adult-type diffuse glioma with isocitrate dehydrogenase (IDH) mutation. Bilateral blindness, as well as bilateral temporal lobe involvement, each has many different causes. However, as demonstrated in this study, adult-type diffuse glioma must be considered a rare cause of concomitant bilateral temporal lobe involvement and blindness.

Introduction

Gliomatosis cerebri (GC) is a diffuse and infiltrative tumoral growth pattern in which the cerebral glioma cells, either isocitrate dehydrogenase (IDH) mutant or wild-type, affect more than 2 brain lobes, most commonly frontotemporal lobes [1,2]. GC is rare and affects all age groups, with the mean age of diagnosis being 43.6 years. The median overall survival is 18.5 months due to no definitive treatment [3,4]. GC is classified as type I (classic type accounting for more than two-thirds of GC cases) when no obvious mass is present or type II when a diffuse infiltrative pattern of involvement coexists with a well-defined enhancing mass-like lesion [2].

Here we present a 35-year-old male patient with a history of bilateral blindness, headache, seizure, and bilateral temporal lobe involvement on MRI who was primarily treated with aciclovir for HSE but later diagnosed as GC, as the complementary investigation results became available. This is the third case of GC being reported, which presented with blindness. We reviewed previous studies, discussed the differential diagnosis, and finally explained the underlying pathophysiology of blindness in GC

Case presentation

A 35-year-old male heroin user from a drug rehabilitation center presented with a 4-month history of headaches and a single episode of seizure a day before. His main complaint was a 2-month history of gradual painless progressive deterioration in visual acuity, which acutely worsened in the days prior to hospitalization. There was no past medical history of immunodeficiency, autoimmune disorders, or malignancy. He displayed no signs or symptoms of withdrawal and denied any current drug or alcohol abuse. On admission to the emergency department (ED), his vital signs were normal, and he was conscious and orientated. Neurological examination showed a bilateral reduction in visual acuity (right side: light perception, left side: hand motion) but was otherwise normal. Slit-lamp examination showed bilateral mild to moderate disc swelling. Pupils were mid-size and isochoric with normal reactions to light.

A brain CT scan was performed, showing hypodensity and loss of grey-white matter differentiation in bilateral temporal lobes, which was extended to occipital lobes and centrum semiovale. Although there was neither obvious mass in the brain parenchyma nor midline shift, mild left uncal herniation was seen (Fig. 1). With regards to signs of probable raised intracranial pressure (ICP), corticosteroids and mannitol were given to decrease edema and prevent further clinical deterioration. Given the presentation (recent seizure and hypodensity of temporal lobes) and a possible higher prevalence of HSE in drug users relative to the normal population in the region (according to high-risk behaviors, poor health care, and different ethnicities in these populations, including illegal immigrants), and due to the high mortality rate of HSE and the benefits and safety of the early treatment, the emergency physician decided to commence empirical therapy with intravenous (IV) aciclovir for the patient while the complementary investigation was underway. A lumbar puncture (LP) was also performed, and urine and blood samples were collected for toxin assay. The cerebrospinal fluid (CSF) sample was clear, and the opening pressure was elevated at 38 cm H_20. A brain MRI was performed for a more detailed investigation. This showed abnormal hypersignal intensity on T2 weighted and fluid-attenuated inversion recovery (FLAIR) sequences in the cortex and subcortical white matter of bilateral temporal lobes and insular regions (more severe on the left side), with extension to genu, body, and splenium of the corpus callosum and centrum semiovale. To a lesser degree, the left basal ganglia, left thalamus, optic chiasm, and periventricular white matter of occipital lobes were involved. Affected areas were mildly expanded and distorted, and they had no restriction on the Diffusion Weighted Imaging (DWI). Involved areas did not show enhancement on postcontrast examination, and no hemorrhagic foci were detected on the Susceptibility Weighted Imaging (SWI) (Fig. 2). Cerebrospinal fluid (CSF) analysis showed a mildly increased glucose but was otherwise normal. The toxin assay of urine and blood samples, as well as tests for human immunodeficiency virus (HIV), hepatitis B and C, were all negative. The real-time polymerase chain reaction (RT-PCR) of Herpes simplex virus (HSV) was negative from the CSF sample, so the aciclovir was discontinued. So, HSE and LE were excluded based on incompatible clinical presentation, imaging findings, and laboratory data.

According to bilateral visual impairment, further evaluation with optical coherence tomography (OCT) and visual evoked potentials (VEPs) testing was performed. These showed bilateral increased retinal nerve fiber layer (RNFL) thickness and absent VEP waveforms, respectively (Fig. 3).

Furthermore, due to volume expansion and facilitated diffusion of involved areas, we had to consider a differential diagnosis of neoplastic lesions such as infiltrative low-grade gliomas. Subsequently, brain MRS was performed for further evaluation, in which the Choline level was greatly elevated in some regions, and Choline to NAA ratio reached up to 4.

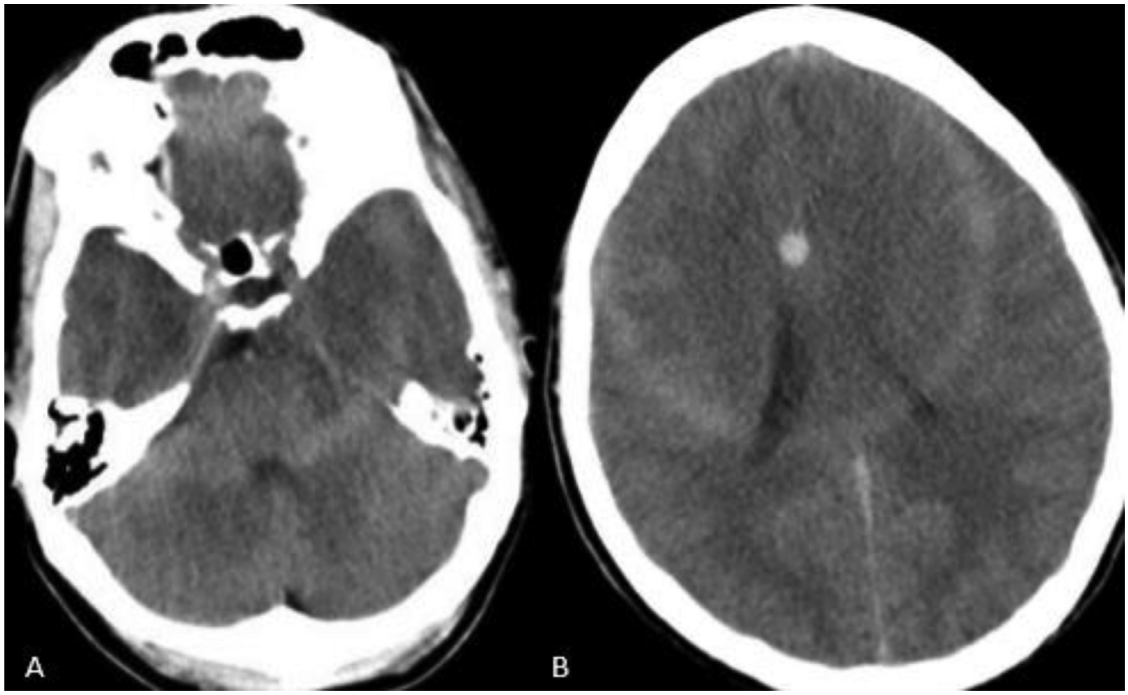

Fig. 1 – Brain CT scan. Hypodensity and loss of gray-white matter differentiation in bilateral temporal lobes (A), white matter hypodensity in bilateral occipital lobes (B). There is a ring artifact in the images.

This favored a diagnosis of the neoplastic nature of this condition (Fig. 4). Raised myo-inositol (MI) peak was also depicted in the obtained MRS imaging results. Following these MRS findings and raised ICP, the patient underwent left temporal lobectomy, and pathology results confirmed the imaging findings and adult-type diffuse glioma was reported. Finally, Immunohistochemistry (IHC) was used to determine tumor marker expression profile and grading (Fig. 5). The patient continued to suffer from blindness and infrequent, mild headaches after the surgery.

Discussion

Bilateral temporal lobe involvement in cross-sectional imaging is not confined to GC, and physicians should rule out the other important differential diagnosis, such as HSE and LE, based on the clinical history, laboratory, and imaging findings [5]. Different imaging modalities and clinical findings which can aid in differentiating these entities are summarized in Table 1.

Progressive visual loss, absence of fever, and a subacute to the chronic course of symptoms were not consistent with the HSE diagnosis. Furthermore, the lack of response to aciclovir therapy increased the probability of GC in this case, although the partial response to aciclovir may be seen in some patients with glioma [6]. Additionally, lack of contrast enhancement on the postcontrast examination despite the nonacute course of the disease, absence of restriction on the DWI and hemorrhage on the SWI, expansion of the involved areas, and involvement of basal ganglia, thalamus, optic chiasm, corpus callosum and bilateral centrum semiovale (indicating infiltrative growth pattern) favors the diagnosis of GC rather than HSE in the conventional MRI. Despite the fact that the MRS spectrum of low-grade gliomas such as GC type 1 may resemble encephalitis, Cho:NAA ratio $\geq$ 2.5 or NAA:Cho ratio $\leq$0.61 suggest a neoplastic nature of the disease rather than non-neoplastic process [7,8]. Our case presented with Chol:NAA ratio of 4. Inositol peak can be seen in 88 % of GC patients and was also present in our case [2].

The lack of underlying malignancy or psychiatric symptoms, extensive extra-limbic involvement, loss of grey-white matter differentiation, presence of a mass effect, and Cho:NAA ratio $\geq$ 2.5 in the affected regions were not compatible with LE.

Castillo et al. [9] propose that low-grade astrocytoma, in comparison to high-grade anaplastic astrocytoma and glioblastoma multiforme (GBM), present with increased levels of MI which is compatible with the findings of our study.

Several acquired diseases may show raised levels of MI, including progressive multifocal Leukoencephalopathy (PML), early-onset Alzheimer's disease, and subacute sclerosing panencephalitis (SSPE) [10,11].

PML is a subacute progressive demyelinating disease caused by oligodendrocyte damage resulting from JC virus infection in immunocompromised patients [12]. Diagnosis is based on the presence of clinical findings and imaging signs, positive CSF JC virus PCR, and exclusion of other diagnoses. It manifests as asymmetrical T2 hyperintense multicentric white matter lesions affecting the U-shaped subcortical fibers and periventricular area. After contrast administration and on DWI, there is usually patchy restricted diffusion and enhancement at the periphery, especially on borders corre-

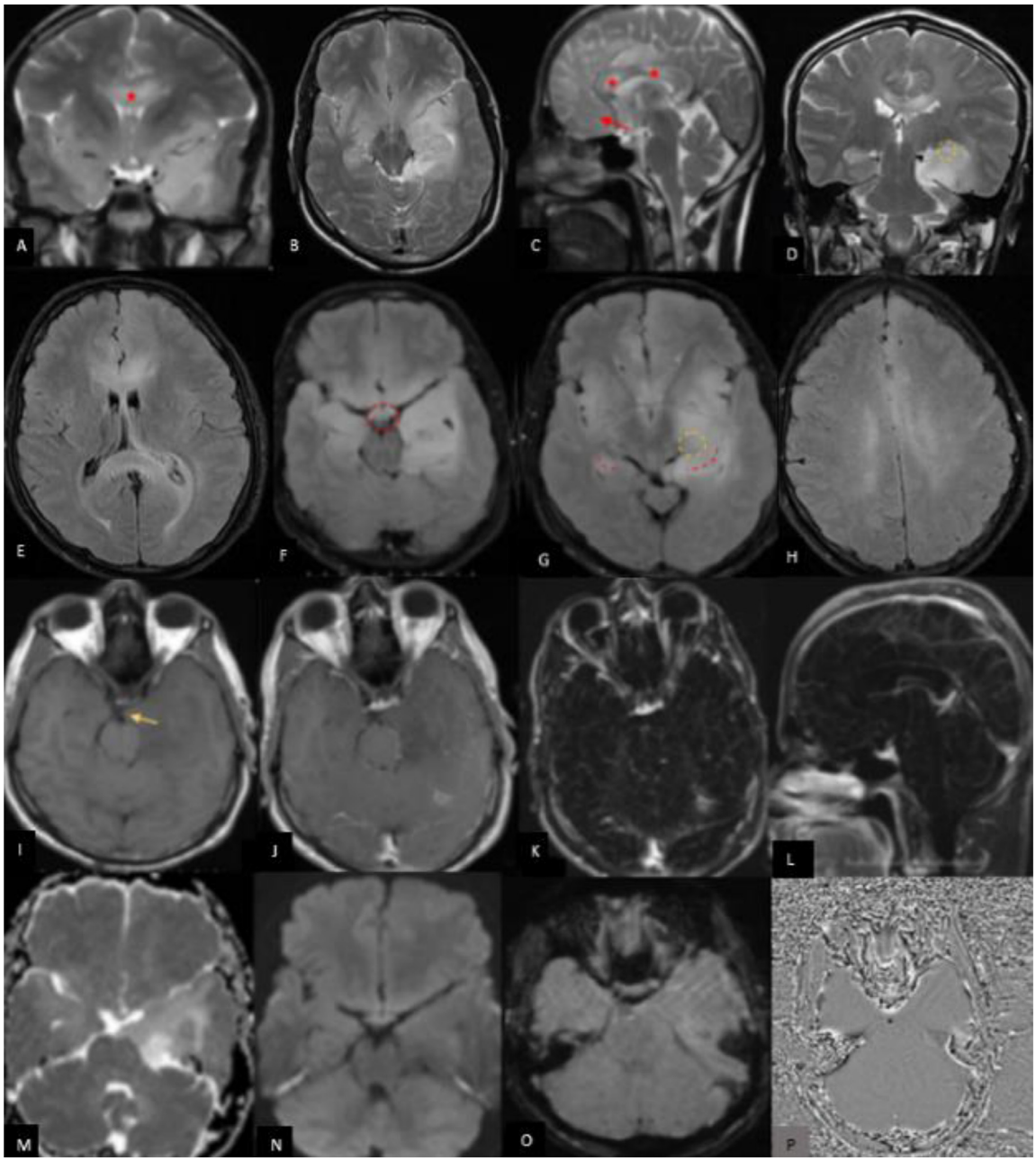

Fig. 2 – Brain MRI. Coronal (A and D), axial (B), and sagittal (C) planes of the brain MRI (T2weighted sequence) showed hyper-signal intensity in bilateral temporal lobes (A, B and D), genu and body of corpus callosum (red stars in A and C) as well as in the optic chiasm (red arrow in C). Hyper-signal regions are mildly expanded (for example, note the gyral thickening of the left medial temporal cortex in B and enlargement of the body of corpus callosum in A). Hyper signal intensity is noted in the anatomic location of the left lateral geniculate body in the posterior coronal plane (yellow circle in D). Selected slices of the FLAIR-axial plane of the brain MRI show Hyper-signal intensity in genu and splenium of the corpus callosum as well as bilateral posterior periventricular white matter (E), bilateral temporal lobes (F and G), the optic chiasm (red circle in F), bilateral insular cortexes, left basal ganglia and left thalamus (G) and also bilateral centrum semiovale (H). Hyper signal intensity is noted in the anatomic location of the left lateral geniculate body (yellow circle in G) and proximal portion of the bilateral optic radiations (dashed red lines in G which is more prominent on the left side). Hyper-signal regions on the T2-weighted and FLAIR exams are mildly hypo-signal on the axial T1-weighted sequence (I). Mild left uncal herniation is seen (yellow arrow in I). Axial T1-weighted sequence with contrast (J), as well as axial and sagittal subtraction images (K and L respectively), show no abnormal leptomeningeal or parenchymal contrast enhancement in the brain. (M and N) There is no obvious diffusion restriction on the DWI/ADC. No Blooming foci are seen in the SWI (O). No abnormal hypo or hyper signal intensity is noted in the filtered phase image (P). So there are no hemorrhagic or calcification foci in the mentioned areas.

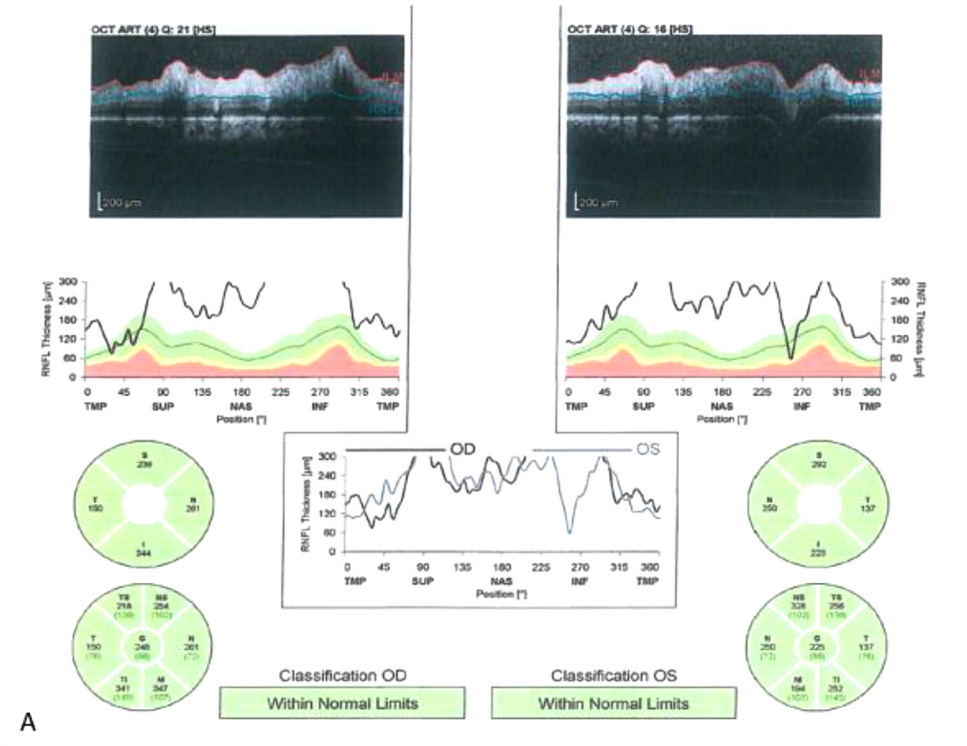

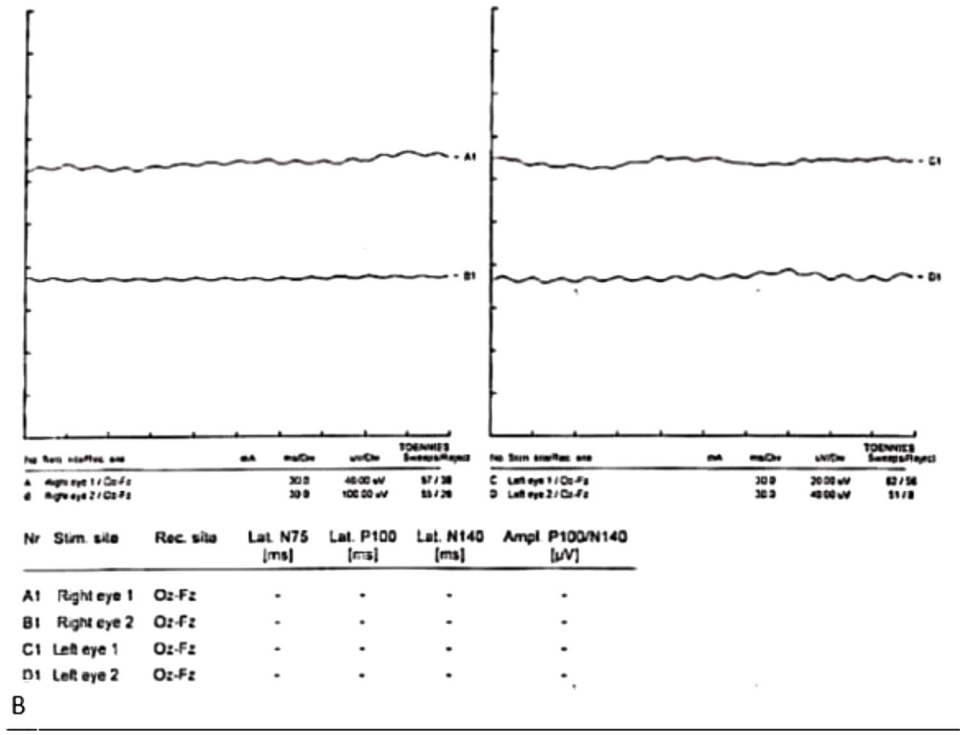

Fig. 3 – OCT and VEP results. (A) OCT shows bilateral increased RNFL thickness accompanied with surface irregularity of this layer indicative of bilateral disc swelling. (B) VEP waveforms are absent bilaterally in favor of severe axonal-type lesions upon the bilateral optic pathways.

Table 1 – Differential diagnoses and their imaging, clinical and laboratory findings.

Differential diagnosis	MRI					MRS	MRP	Clinical presentation	CSF analysis (LP)
	Conventional MRI findings			DWI	SWI				
	Involved areas	T1/T2/FLAIR	Enhancement						
Gliomatosis Cerebri [1,2,38–46]	Usually, 3 or more lobes are involved (with poorly marginated and infiltrative patterns). Temporal lobe (79%)> frontal lobe (73%)> parietal lobe (60%)> occipital lobe (34%) Bilateral involvement of temporal lobes may occur. Extension to the basal ganglia (48%), corpus callosum (49%), or infratentorial structures (29%) is possible. Involvement of parahippocampal gyrus, insular cortex, and extra-limbic structures are more common in GC than in LE.	Iso to hypo signal/ high signal/high signal. Gyral thickening and enlargement of the affected regions are present. Mass effect is more common in GC than HSE and LE.	Minimal (16%-56%) or no enhancement. Enhancement patterns include: focal, multifocal, or nodular. In GC type II, a discrete enhancing mass is present	No restriction. Restriction on the DWI may be seen if GC type II with a discrete high-grade mass is present	No hemorrhagic foci (if the tumor is low-grade)	Increased choline to creatinine (Cho:Cr) ratio as the most sensitive and specific measure; raised choline to N-acetyl aspartate (Cho:NAA) ratio; decreased NAA:Cr ratio; a significant rise in myo-inositol; 2-Hydroxyglutarate (2-HG) peak in IDH-mutant patients in 2.25 ppm with a cutoff value of 1.76 mM; It is worth mentioning that a higher Cho:NAA ratio does not always indicate higher grades of tumor (like in our case)	Low or normal relative cerebral blood volume (rCBV) without any hyperplasia of vessels is seen in low-grade gliomas. Much higher in high-grade ones with a differentiating border of 0.63; although rCBVt (intratumoral) Value of 1.7 is also mentioned to differentiate LGG from HGG; CBV values higher than 2.3 is correlated with the IDH-wild type. Mean ± SD for 7 GC cases: 1.02 ± 0.42	Seizures (50%), headache (36%), cognitive decline (32%), focal motor deficits (32%), cerebellar symptoms (21%), visual disturbance and papilledema due to raised ICP (15%), behavioral change (13%), psychiatric symptoms (8%)	Nonspecific may be normal or mild pleocytosis, increased protein level and raised opening pressure may be present.

(*continued on next page*)

Table 1 (*continued*)

Differential diagnosis	MRI					MRS	MRP	Clinical presentation	CSF analysis (LP)
	Conventional MRI findings			DWI	SWI				
	Involved areas	T1/T2/FLAIR	Enhancement						
HSV Encephalitis [47–53]	In immunocompetent patients, unilateral or asymmetrically bilateral involvement of medial temporal lobes, inferolateral frontal lobes, insular cortexes, and cingulate gyrus occurs (with sparing of basal ganglia). Mammillary bodies, hypothalamus, and diffuse white matter involvement is a rare condition but is possible. In immunocompromised patients, extensive involvement is common, even in the brainstem.	hypo signal/high signal/high signal. Hemorrhage alters the signal pattern, depending on the stage (for example, high signal on the T1 weighted sequence and low signal on T2 weighted sequence in the early sub-acute phase)	It may be restricted primarily in the acute phase (more sensitive than T2 weighted sequence), facilitated with high ADC in chronic herpetic encephalitis	It may be restricted primarily in the acute phase (more sensitive than T2 weighted sequence), facilitated with high ADC in chronic herpetic encephalitis	+/-Petechial Hemorrhagic foci	Decreased NAA:Cr ratio and increased Cho:Cr ratio; Significantly reduced NAA and slightly reduced Cr; substantially raised lactate (Lac), increased choline levels, and normal myo-inositol level. These changes are usually transient, and normalization occurs parallel to the clinical improvement.	Increased cerebral blood flow (rCBF) and rCBV Mean CBF values for 17 patients were 2.68 ± 0.54 in the acute, 2.42 ± 0.52 in the subacute, and 0.87 ± 0.30 in the chronic stage.	Mostly constitutional, including fever and headache, but sometimes neural deficit, seizure, or impaired cognition occurs. Visual disturbance is rare in encephalitis, especially as a first sign. Rapid progression of symptoms favors this diagnosis.	High protein levels and pleocytosis
Limbic (autoimmune) Encephalitis [54–56,46,57]	The mesial temporal lobe and limbic system are affected. Basal ganglia can be involved. Bilateral involvement of temporal lobes is more common in LE than in GC or HSE.	Iso signal/ High signal/ High signal. Maintenance of Differentiation between the gray and white matter is in favor of LE rather than GC	Sometimes patchy	Usually no restriction *LE can show transient restriction in patients with seizures due to postictal white matter changes	No Hemorrhagic foci	In a paraneoplastic-type patient, elevated choline and myo-inositol levels with a lactate peak and a decrease in NAA level were seen.	-	Either para-neoplastic (for example, small cell lung cancer) or non-neoplastic with changed mental status, psychiatric problems, seizure, and memory disturbance. More chronic clinical courses than HSE	Pleocytosis, elevated protein, and the presence of the oligoclonal band and specific autoantibodies

2-HG, 2-Hydroxyglutarate; ADC, Apparent diffusion coefficient; Cho, choline; Cr, creatinine; CSF, cerebrospinal fluid; DWI, Diffusion Weighted Imaging; FLAIR, fluid-attenuated inversion recovery; GC, Gliomatosis cerebri; HGG, high grade glioma; HSE, Herpes simplex encephalitis; HSV, Herpes simplex virus; ICP, intracranial pressure; IDH, isocitrate dehydrogenase; Lac, lactate; LE, limbic encephalitis; LGG, low grade glioma; LP, lumbar puncture; MRI, magnetic resonance imaging; MRP, Magnetic Resonance Perfusion; MRS, magnetic resonance spectroscopy; NAA, N-acetyl aspartate; rCBF, relative cerebral blood flow; rCBV, relative cerebral blood volume; rCBVt relative cerebral blood volume intratumoral; SWI, Susceptibility weighted imaging.

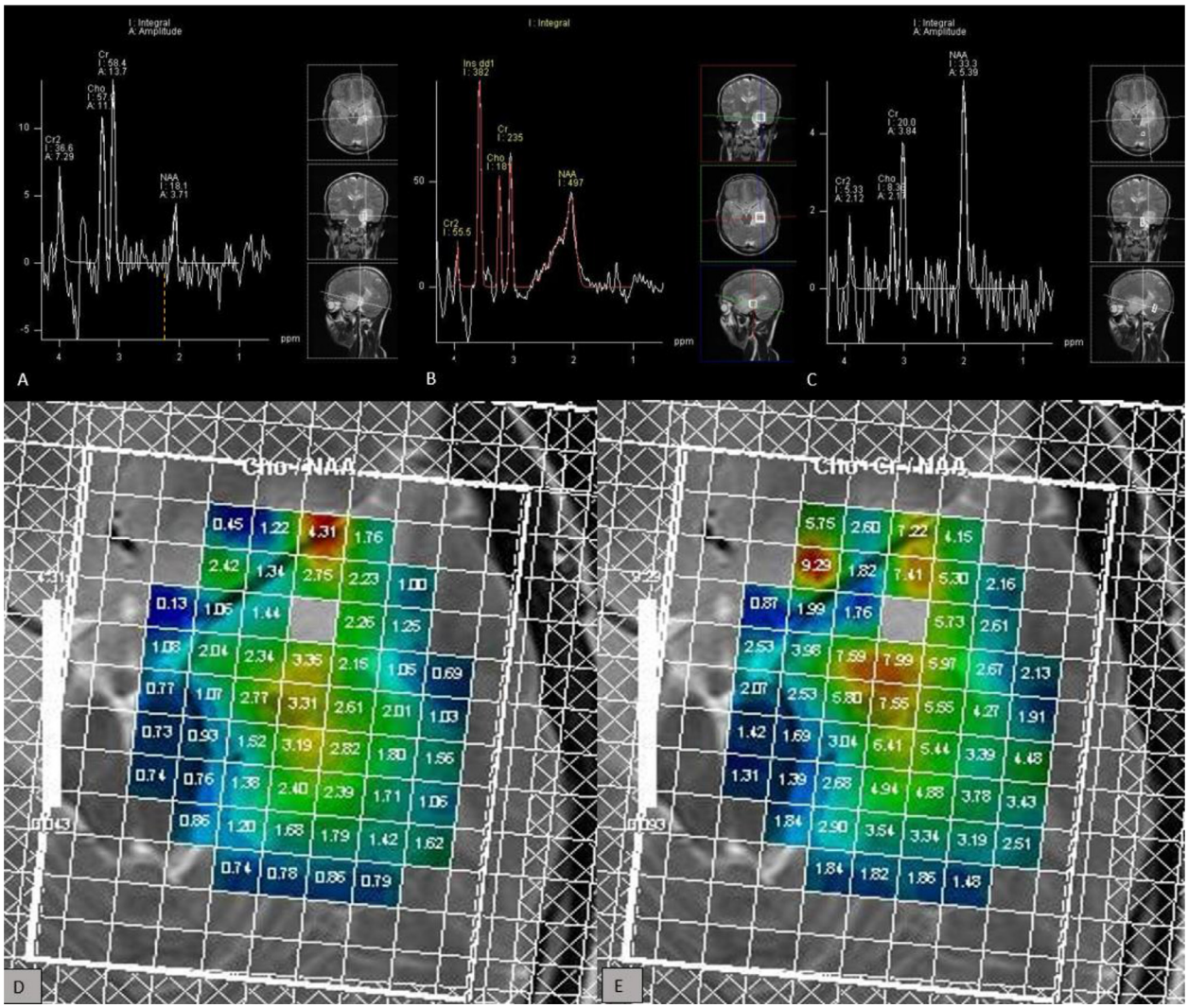

Fig. 4 – Brain MRS. (A) MR spectroscopy of the left temporal hyper-signal area shows Choline peak and markedly reduced NAA levels. There is a suspicious peak at 2.25 ppm (yellow dashed line), which could be in favor of the 2HG metabolite (seen in IDH-mutant gliomas), but postprocessing and advanced MR spectroscopy should be performed to confirm that which was not available. (B) There is an inositol peak at 3.5 ppm in the left temporal area. (C) MR spectroscopy of the ipsilateral normal brain parenchyma. (D and E) The MRS map (D: Chol/NAA, E: Chol+Cr/ NAA) shows an increased Chol/NAA ratio up to 4.3 and Chol+Cr/NAA ratio up to 9.29.

sponding to active demyelination [13–15]. Lack of a previous history of immunodeficiency along with negative test result of HIV, absence of a typical pattern of enhancement and restriction seen in PML as well as the presence of mass effect and cortical involvement lessens the possibility of PML in our patient. Moreover, markedly raised choline and lipid, substantially reduced NAA, and the presence of lactate peak comprise MRS results of PML, which raised lipid/lactate levels were not seen in our case [16].

Extensive T2/FLAIR hyper signal intensity in the mentioned areas and lack of gyral atrophy or ventricular enlargement diminished AD probability [17,18].

SSPE primarily impacts individuals during childhood or youth who have a history of measles infection preceding the onset of the disease (which was not present in our case) [19,20]. The acute phases mainly present as asymmetrical patches of white matter involvement in the temporoparietal region, and severe cases may reveal callosal and brainstem involvement [21]. The possibility of cortical blindness due to the involvement of optic radiations, lack of restricted diffusion, and contrast enhancement were other similarities between SSPE and our case, but grey matter involvement and mass effect were not consistent with the diagnosis of SSPE [21–23]. Moreover, decreased NAA/Cr, increased Chol/Cr, and raised lactate and MI levels occur in stage III of SSPE which the patient is usually in a coma, and cerebral, cerebellar, or brain stem atrophy has occurred [24].

Other differential diagnoses we considered for an IV drug user with extensive involvement of white matter were toxic leukoencephalopathy, lymphomatosis cerebri, HIV

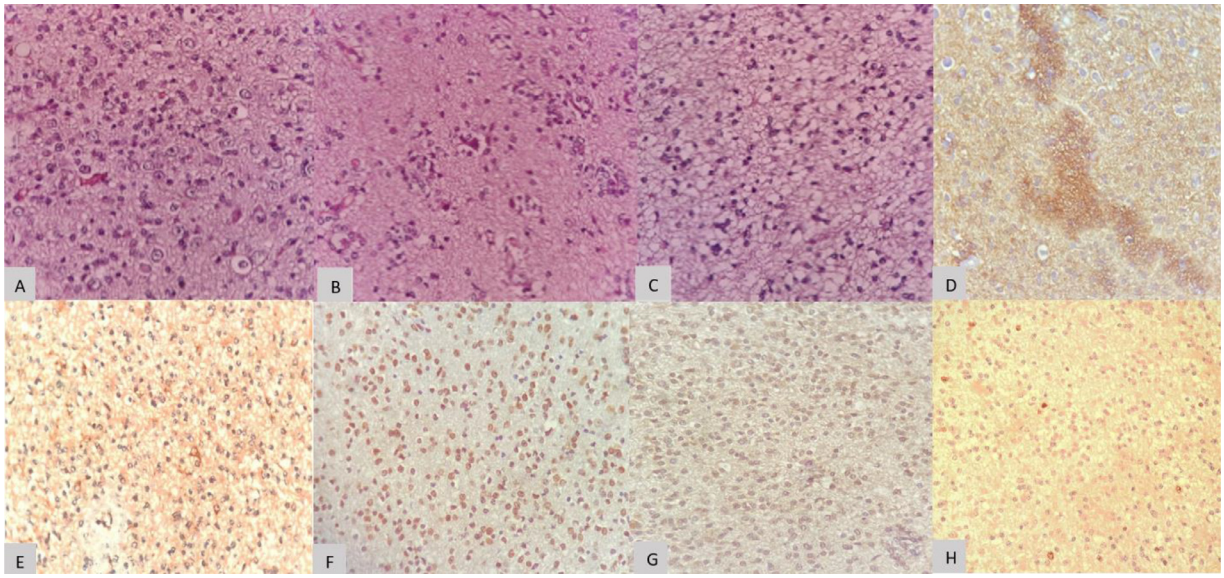

Fig. 5 – Pathology and IHC results (all images taken with magnification 100X). (A–C) Increased glial cellularity and accumulation of tumor cells (around the neurons, known as perineural satellitosis) with oval-shaped astrocytic nuclei and variable appearance of tumor cytoplasm and glial fibrillary processes in the brain tissue are seen, suggesting a diffuse astrocytoma. There is no obvious evidence of necrosis and microvascular proliferation. Astrocytes stained positively for GFAP (D), IDH1(E), ATRX (F), and P53 (G), whereas Ki67 (H) immunostaining reveals around 5% growing tumor cells. The results were compatible with a diagnosis of grade II astrocytoma (low-grade).

encephalopathy, and primary angiitis of the central nervous system (PACNS). We ruled out these differential diagnoses with laboratory results and lack of their specific imaging findings.

The prominent clinical feature of our case was bilateral blindness, which necessitates further investigation. Raised ICP can lead to bilateral vision loss, papilledema, RNFL thickening in OCT [25], and latency in VEP waveforms [26]. However, blindness occurs in longstanding papilledema with optic disc atrophy [27,28], which was not present in our case. Moreover, bilateral obliteration of VEP waveforms is not explained by increased ICP alone and usually occurs in bilateral optic nerve damage, bilateral severe ocular disease, and less commonly in cases with chiasmatic or extensive bilateral retrochiasmatic lesions such as gliomas [29,30]. Additionally, the involvement of the optic nerves or optic tract affects pupillary reflex, unlike the involvement of the lateral geniculate body (LGB) or optic radiation (OR) [31,32].

According to these data and also T2 hyper signal intensity of optic chiasm and estimated locations of OR/LGB in MRI (Figs. 2 D, F, and G), infiltration of these regions by glioma cells constitutes a stronger reason for unpredicted visual loss in the presented case, although chronic raised ICP may also have a role. Bilateral anopsia is either due to tumors emerging in the chiasma or infiltration or mass effect of tumoral tissue on pre- and postchiasmatic pathways on both sides [33,34], similar to what probably happened in this case.

Only 2 cases have been reported of a GC patient presenting with blindness; the first one was a case with progressive damage to optic chiasma, optic nerves, and septum pellucidum and was reported in 1996, who was misdiagnosis as multiple sclerosis based on the imaging findings led to vision deterioration and emerging additional bilateral ocular findings, including mydriasis, papilledema, and temporal pallor [35]. The second case was reported in 2020, A 45-year-old patient presenting with a history of generalized tonic-clonic seizures and gradual, painless loss of vision in both eyes. The patient reported an inability to perceive light in both eyes, and reactions of his pupils to light were sluggish. With papilledema and absent foveal reflex, an initial diagnosis of optic neuritis secondary to demyelinating disorder or nonarteritic ischemic optic neuropathy was made. A later MRI scan revealed signs of a diffuse infiltrative glial tumor in favor of GC [36]. A detailed comparison of these cases is available in supplementary material 1.

Diffusion tensor imaging (DTI) is an MRI modality that specifically detects white matter fiber distortion or infiltration [37]. DTI can be used in similar cases for identifying and confirming the optic pathway's involvement. Hence, the inability to use DTI imaging modality was the main limitation of our current case report.

Conclusion

In this publication, we presented a gliomatosis cerebri (GC) case with bilateral blindness, a rare disease with a rare complication. Further evaluations with MR spectroscopy, MR perfusion imaging, and finally, stereotactic biopsy with immunohistochemistry (IHC) staining are necessary in GC cases with inexplicable imaging and clinical findings.

CRediT author statement

Conceptualization: Masih Falahatian Writing Original draft, review, and editing: Amirreza Jahanshahi, Sareh Salarinejad, Saeed Oraee-Yazdani, Yasaman Chehresonboll, Soroush Morsali, Ali Jafarizadeh, Masih Falahatian, Faezeh Rahimi, Mehran Jaberinezhad.

Patient consent

We claim and confirm that written, informed consent and full permission for publication, reproduction, broadcast and other use of our case scientific information (like past medical histories, present illness, photographs, recordings, other audiovisual material) was obtained from the patient and his first degree family.

Supplementary materials

Supplementary material associated with this article can be found, in the online version, at doi:10.1016/j.radcr.2023.05.037.

REFERENCES

[1] Ranjan S, Warren KE. Gliomatosis cerebri: current understanding and controversies. Front Oncol 2017;7:165.
[2] Georgakis MK, Tsivgoulis G, Spinos D, Dimitriou NG, Kyritsis AP, Herrlinger U, et al. Clinical, neuroimaging and histopathological features of gliomatosis cerebri: a systematic review based on synthesis of published individual patient data. J Neuro-Oncol 2018;140(2):467–75.
[3] Georgakis MK, Spinos D, Pourtsidis A, Psyrri A, Panourias IG, Sgouros S, et al. Incidence and survival of gliomatosis cerebri: a population-based cancer registration study. J Neuro-Oncol 2018;138(2):341–9.
[4] Chen S, Tanaka S, Giannini C, Morris J, Yan ES, Buckner J, et al. Gliomatosis cerebri: clinical characteristics, management, and outcomes. J Neuro-Oncol 2013;112(2):267–75.
[5] Eran A, Hodes A, Izbudak I. Bilateral temporal lobe disease: looking beyond herpes encephalitis. Insights Imag 2016;7(2):265–74.
[6] Piper K, Foster H, Gabel B, Nabors B, Cobbs C. Glioblastoma mimicking viral encephalitis responds to acyclovir: a case series and literature review. Front Oncol 2019;9:8.
[7] Abdelgawad MS, Kayed MH, Reda MIS, Abdelzaher E, Farhoud AH, Elsebaie N. Contribution of advanced neuro-imaging (MR diffusion, perfusion and proton spectroscopy) in differentiation between low grade gliomas GII and MR morphologically similar non neoplastic lesions. Egypt J Radiol Nucl Med 2022;53(1):1–11.
[8] Horská A, Barker PB. Imaging of brain tumors: MR spectroscopy and metabolic imaging. Neuroimag Clin 2010;20(3):293–310.
[9] Castillo M, Smith JK, Kwock L. Correlation of myo-inositol levels and grading of cerebral astrocytomas. AJNR Am J Neuroradiol 2000;21(9):1645–9.
[10] Provencher SW. Automatic quantitation of localized in vivo 1H spectra with LCModel. NMR in Biomed 2001;14(4):260–4.
[11] Jack CR Jr, Holtzman DM. Biomarker modeling of Alzheimer's disease. Neuron 2013;80(6):1347–58.
[12] Sakai M, Higashi M, Fujiwara T, Uehira T, Shirasaka T, Nakanishi K, et al. MRI imaging features of HIV-related central nervous system diseases: diagnosis by pattern recognition in daily practice. Jpn J Radiol 2021;39(11):1023–38.
[13] Alleg M, Solis M, Baloglu S, Cotton F, Kerschen P, Bourre B, et al. Progressive multifocal leukoencephalopathy: MRI findings in HIV-infected patients are closer to rituximab- than natalizumab-associated PML. Eur Radiol 2021;31(5):2944–55.
[14] Garrels K, Kucharczyk W, Wortzman G, Shandling M. Progressive multifocal leukoencephalopathy: clinical and MR response to treatment. AJNR Am J Neuroradiol 1996;17(3):597–600.
[15] Berger JR, Levy RM, Flomenhoft D, Dobbs M. Predictive factors for prolonged survival in acquired immunodeficiency syndrome-associated progressive multifocal leukoencephalopathy. Ann Neurol 1998;44(3):341–9.
[16] Iranzo A, Moreno A, Pujol J, Martí-Fàbregas J, Domingo P, Molet J, et al. Proton magnetic resonance spectroscopy pattern of progressive multifocal leukoencephalopathy in AIDS. J Neurol Neurosurg Psychiatry 1999;66(4):520–3.
[17] Zhai S, Brew BJ. Progressive multifocal leukoencephalopathy. Handb Clin Neurol 2018;152:123–37.
[18] Chandra A, Dervenoulas G, Politis M. Magnetic resonance imaging in Alzheimer's disease and mild cognitive impairment. J Neurol 2019;266(6):1293–302.
[19] Garg RK. Subacute sclerosing panencephalitis. Postgrad Med J 2002;78(916):63–70.
[20] Herath H, Nandasiri S, Chandrakumara A, Jayamaha J, Senanayake S, Goonaratne K. Subacute sclerosing panencephalitis: a rare cause of acute cortical visual impairment in an adult. Trop Doct 2020;50(4):354–8.
[21] Sener RN. Subacute sclerosing panencephalitis findings at MR imaging, diffusion MR imaging, and proton MR spectroscopy. AJNR Am J Neuroradiol 2004;25(5):892–4.
[22] Senbil N, Aydin OF, Orer H, Gürer YK. Subacute sclerosing panencephalitis: a cause of acute vision loss. Pediatr Neurol 2004;31(3):214–17.
[23] Barthwal S, Kaur N, Kaur R, Zaidi R, Randev S. Magnetic resonance imaging in subacute sclerosing panencephalitis: two case reports and review of literature. Cureus 2021;13(10):e19161.
[24] Alkan A, Sarac K, Kutlu R, Yakinci C, Sigirci A, Aslan M, et al. Early- and late-state subacute sclerosing panencephalitis: chemical shift imaging and single-voxel MR spectroscopy. AJNR Am J Neuroradiol 2003;24(3):501–6.
[25] Skau M, Yri H, Sander B, Gerds TA, Milea D, Jensen R. Diagnostic value of optical coherence tomography for intracranial pressure in idiopathic intracranial hypertension. Graefes Arch Clin Exp Ophthalmol 2013;251(2):567–74.
[26] Canac N, Jalaleddini K, Thorpe SG, Thibeault CM, Hamilton RB. Review: pathophysiology of intracranial hypertension and noninvasive intracranial pressure monitoring. Fluids Barriers of the CNS 2020;17(1):40.
[27] Rowe FJ. Assessment of visual function in idiopathic intracranial hypertension. Br J Neurosurg 2011;25(1):45–54.
[28] Schirmer CM, Hedges TR. Mechanisms of visual loss in papilledema. Neurosurg Focus FOC 2007;23(5):E5.
[29] Yu M, Creel D. Visually evoked potentials. Handb Clin Electrophysiol Vision 2019;1:19–28.
[30] Drislane FW. Visual evoked potentials. In: Blum AS, Rutkove SB, editors. The clinical neurophysiology primer. Totowa, NJ: Humana Press; 2007. p. 461–73.

[31] Swienton DJ, Thomas AG. The visual pathway—functional anatomy and pathology. Semin Ultrasound, CT and MRI 2014;35(5):487–503.
[32] Khurana AK. Neuro-ophthalmology. Jaypee, The Health Sciences Publisher 2015. New Delhi, India, Second Edition, ISBN 9789351527824.
[33] Nguyen HN, Vo KB, Howard S, Salamat MS, Rowely H, Robins HI. Vision loss in glioblastoma: disease mimicking presumed therapeutic toxicity. Neuro-Oncol Pract 2018;5(4):223–6.
[34] Lee AG, Charoenkijkajorn C, Karimaghaei C, Pakravan M, Lee VA, Al-Zubidi N. Neuro-ophthalmic manifestations of glioblastoma multiforme. J Neuroophthalmol;40:e31-e48
[35] Felsberg G, Glass J, Tien R, McLendon R. Gliomatosis cerebri presenting with optic nerve involvement: MRI. Neuroradiology 1996;38(8):774–7.
[36] Sekar P, Rajarajeswary P, Prasanth H, Ishwarya T, Srinivasan R, Kannan R. Gliomatosis cerebri - a rare cause of bilateral blindness. TNOA J Ophthalm Sci Res 2020;58(4):304–6.
[37] Davanian F, Faeghi F, Shahzadi S, Farshifar Z. Diffusion tensor imaging for glioma grading: analysis of fiber density index. Basic Clin Neurosci 2017;8(1):13.
[38] Shin YM, Chang KH, Han MH, Myung NH, Chi J, Cha SH, et al. Gliomatosis cerebri: comparison of MR and CT features. AJR Am J Roentgenol 1993;161(4):859–62.
[39] Bendszus M, Warmuth-Metz M, Klein R, Burger R, Schichor C, Tonn JC, et al. MR spectroscopy in gliomatosis cerebri. Am J Neuroradiol 2000;21(2):375–80.
[40] Zikou A, Alexiou G, Argyropoulou M. Advanced MR imaging techniques in the diagnosis of intra-axial brain tumors. Neurooncol-Newer Develop 2016;1:165–81 IntechOpen.
[41] Suh CH, Kim HS, Jung SC, Choi CG, Kim SJ. 2-Hydroxyglutarate MR spectroscopy for prediction of isocitrate dehydrogenase mutant glioma: a systemic review and meta-analysis using individual patient data. Neuro-Oncol 2018;20(12):1573–83.
[42] Yang S, Wetzel S, Cha S. Dynamic contrast-enhanced T2*-weighted MR imaging of gliomatosis cerebri. Am J Neuroradiol 2002;23(3):350–5.
[43] Kumar Y, Gupta N, Mangla M, Hooda K, Mangla R. Comparison between MR perfusion and 18F-FDG PET in differentiating tumor recurrence from nonneoplastic contrast-enhancing tissue. Asian Pac J Cancer Prev 2017;18(3):759–63.
[44] Hasan A-MS, Hasan AK, Megally HI, Khallaf M, Haseib A. The combined role of MR spectroscopy and perfusion imaging in preoperative differentiation between high-and low-grade gliomas. Egypt J Radiol Nucl Med 2019;50(1):1–9.
[45] Shakir TM, Fengli L, Chenguang G, Chen N, Zhang M, Shaohui M. 1H-MR spectroscopy in grading of cerebral glioma: a new view point, MRS image quality assessment. Acta Radiologica Open 2022;11(2):20584601221077068.
[46] Blinder T, Lewerenz J. Cerebrospinal fluid findings in patients with autoimmune encephalitis—a systematic analysis. Front Neurol 2019;10:804.
[47] Bulakbasi N, Kocaoglu M. Central nervous system infections of herpesvirus family. Neuroimag Clin N Am 2008;18(1):53–84.
[48] Stahl JP, Mailles A. Herpes simplex virus encephalitis update. Curr Opin Infect Dis 2019;32(3):239–43.
[49] Sawlani V. Diffusion-weighted imaging and apparent diffusion coefficient evaluation of herpes simplex encephalitis and Japanese encephalitis. J Neurol Sci 2009;287(1-2):221–6.
[50] Sämann PG, Schlegel J, Müller G, Prantl F, Emminger C, Auer DP. Serial proton MR spectroscopy and diffusion imaging findings in HIV-related herpes simplex encephalitis. Am J Neuroradiol 2003;24(10):2015–19.
[51] Li R, Shi P-A, Liu T-F, Li Y, Wang Y, Wu K, et al. Role of 3D pseudocontinuous arterial spin-labeling perfusion in the diagnosis and follow-up in patients with herpes simplex encephalitis. Am J Neuroradiol 2019;40(11):1901–7.
[52] Ono Y, Manabe Y, Nishimura H, Kono S, Narai H, Omori N, et al. Unusual progression of herpes simplex encephalitis with basal ganglia and extensive white matter involvement. Neurol Int 2009;1(1):e9.
[53] Da Rocha A, Nunes R, Maia A, Do Amaral L. Recognizing autoimmune-mediated encephalitis in the differential diagnosis of limbic disorders. Am J Neuroradiol 2015;36(12):2196–205.
[54] Oyanguren B, Sánchez V, González F, de Felipe A, Esteban L, López-Sendón J, et al. Limbic encephalitis: a clinical-radiological comparison between herpetic and autoimmune etiologies. Eur J Neurol 2013;20(12):1566–70.
[55] Isik N, Candan F, Dincer A, Dama D, Seleker T, Aydin I. Serial cranial MR imaging and single voxel proton MR spectroscopy in paraneoplastic limbic encephalitis. Eur J Radiol Extra 2004;50(1):1–7.
[56] Ismail II, Alnaser F, JY Al-Hashel. Seronegative limbic encephalitis manifesting as subacute amnestic syndrome: a case report and review of the literature. J Med Case Rep 2021;15(1):1–6.
[57] Zoccarato M, Valeggia S, Zuliani L, Gastaldi M, Mariotto S, Franciotta D, et al. Conventional brain MRI features distinguishing limbic encephalitis from mesial temporal glioma. Neuroradiology 2019;61(8):853–60.